New Steric Hindrance Approach Employing the Hybrid Ligand 2-Aminomethylpiperidine for Diminishing Dynamic Motion Problems of Platinum Anticancer Drug Adducts Containing Guanine Derivatives

Hing C. Wong,[†] Raymond Coogan,[‡] Francesco P. Intini,[‡] Giovanni Natile,*[,‡] and Luigi G. Marzilli*[,†]

Department of Chemistry, Emory University, Atlanta, Georgia 30322, and Dipartimento Farmaco-Chimico, Università degli Studi di Bari, 70125 Bari, Italy

Received August 18, 1998

A fundamental problem obscuring the role of the ammine and primary amine groups in the activity of clinically used Pt anticancer drugs is the dynamic character of the adducts with DNA and DNA constituents. Dynamic motion is slower in analogues containing only secondary or tertiary amines, but such agents are not used clinically. Recently we found that enclosing the N center within a piperidine (pip) ring greatly reduces dynamic motion. In this work, we test the hypothesis that a diamine with only one pip ring, 2-aminomethylpiperidine (**pipen**), would slow dynamic motion enough for insightful study of adducts with one site (cis to the primary amine) closely reflecting the coordination environment of clinically used drugs. Racemic **pipen** was prepared and resolved by improved methods. $PtCl_2$(**pipen**) synthesized with the **pipen** enantiomer having an *R* configuration of the asymmetric carbon (determined on the basis of the $[\alpha]_D$ sign) has the *S* stereochemistry at the N asymmetric center. In the adduct (*S*,*R*)-**pipen**Pt(5′-GMP)$_2$, restricted rotation of the two nonequivalent N7-coordinated 5′-GMP's about the Pt−N7 bonds potentially could lead to two head-to-tail (ΛHT and ΔHT) and two head-to-head (HH_1 and HH_2) atropisomers. However, 1D and 2D NOESY NMR data at pH ∼ 3 indicated the dominance of the two HT atropisomers in a ΛHT:ΔHT ratio of 2:1. Deprotonation of the phosphate group (pH 7) further stabilized the ΛHT form, and the CD signal had the shape characteristic of a ΛHT form with a positive peak at ∼280 nm. However, at pH 9.5, where the 5′-GMP N1H was largely deprotonated, the NMR spectrum and the ∼280 nm CD peak both revealed that the ΛHT form had decreased. When the pH was jumped down to 6.9, the NMR signals of the ΛHT form and the ∼280 nm CD peak increased with a half-time of ∼3 min. Thus, the pip ring lengthens the atropisomerization time from seconds for **ethylenediamine**Pt(5′-GMP)$_2$ to minutes for (*S*,*R*)-**pipen**Pt(5′-GMP)$_2$. This pH jump experiment indicates that the signs of the CD signal are opposite for the ΛHT and ΔHT forms. Changes with pH in both the relative abundance and shifts of the H8 signals of the ΛHT and ΔHT forms correlated with an increase in hydrogen bonding by the phosphate group of the 5′-GMP cis to the primary amine. The hydrogen bonding changes the 5′-GMP base tilt and hence the H8 chemical shift. Such information is not obtainable on 5′-GMP adducts of clinically used anticancer drugs.

Introduction

Since the discovery of its anticancer activity, many new analogues of *cis*-$PtCl_2(NH_3)_2$ (cisplatin) have been synthesized and tested for biological activity, and some of these compounds are now well-established anticancer drugs.[1−3] Heterocyclic, alicyclic, straight- and branched-chain alkylamines, and chelating diamines all give compounds with appreciable activity; moreover, these carrier amine ligands appear to modulate the anticancer properties of this class of drugs. Activity is usually lost or diminished if the primary or secondary amines on platinum are replaced by tertiary amines.[4] Although the precise mechanism of action of these Pt drugs is not completely understood, the drugs are known to target DNA primarily by forming bifunctional adducts involving the N7 of guanine (**G**) residues (Chart 1).[5] The important dependence of activity on the presence of NH groups in the carrier ligand has led to the hypothesis that **G** O6−NH[6−9] and/or phosphate−NH[8−15] intramolecular hydrogen bonding within the Pt−DNA adduct influences structure and hence activity.

There are many other hypothetical roles for the carrier ligand. DNA−carrier ligand hydrogen bonding could also affect the

[†] Emory University.
[‡] Università degli Studi di Bari.

(1) Bloemink, M. J.; Reedijk, J. In *Metal Ions in Biological Systems*; Sigel, A., Sigel, H., Eds.; Marcel Dekker: New York, 1996; Vol. 32; p 641.
(2) Reedijk, J. *Chem. Commun.* **1996**, 801.
(3) Pasini, A.; Zunino, F. *Angew. Chem., Int. Ed. Engl.* **1987**, *26*, 615.
(4) Sundquist, W. I.; Lippard, S. J. *Coord. Chem. Rev.* **1990**, *100*, 293.
(5) Pinto, A. L.; Lippard, S. J. *Biochim. Biophys. Acta* **1985**, *780*, 167.
(6) Sherman, S. E.; Gibson, D.; Wang, A. H. J.; Lippard, S. J. *J. Am. Chem. Soc.* **1988**, *110*, 7368.
(7) Xu, Y.; Natile, G.; Intini, F. P.; Marzilli, L. G. *J. Am. Chem. Soc.* **1990**, *112*, 8177.
(8) Kiser, D.; Intini, F. P.; Xu, Y.; Natile, G.; Marzilli, L. G. *Inorg. Chem.* **1994**, *33*, 4149.
(9) Guo, Z.; Sadler, P. J.; Zang, E. *Chem. Commun.* **1997**, 27.
(10) Berners-Price, S. J.; Frey, U.; Ranford, J. D.; Sadler, P. J. *J. Am. Chem. Soc.* **1993**, *115*, 8649.
(11) Berners-Price, S. J.; Ranford, J. D.; Sadler, P. J. *Inorg. Chem.* **1994**, *33*, 5842.
(12) Berners-Price, S. J.; Frenkiel, T. A.; Ranford, J. D.; Sadler, P. J. *J. Chem. Soc., Dalton Trans.* **1992**, 2137.
(13) Bloemink, M. J.; Heetebrij, R. J.; Inagaki, K.; Kidani, Y.; Reedijk, J. *Inorg. Chem.* **1992**, *31*, 4656.
(14) Reedijk, J. *Inorg. Chim. Acta* **1992**, *198−200*, 873.
(15) Fouts, C. S.; Marzilli, L. G.; Byrd, R. A.; Summers, M. F.; Zon, G.; Shinozuka, K. *Inorg. Chem.* **1988**, *27*, 366.

10.1021/ic980987u CCC: $18.00
Published on Web 02/05/1999

Chart 1. 5′-GMP Structure and Numbering Scheme with the Definition of Two Types of Arrows Used To Sketch **G** Derivatives[a]

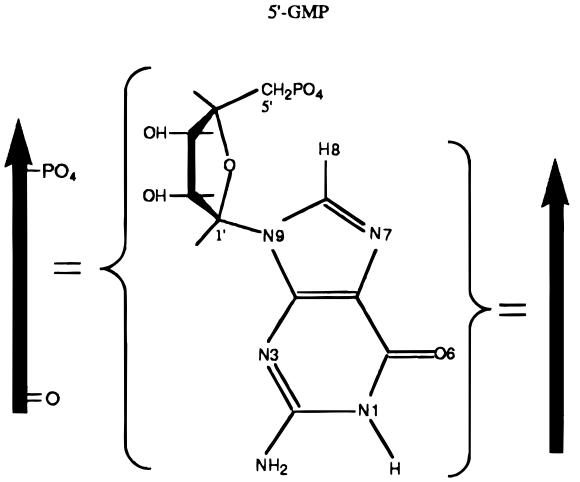

[a] Arrow on right defines the base directional properties (see Figure 1 caption). Arrow on left is used below to depict hydrogen-bonding motifs involving the phosphate group or O6 of 5′-GMP.

initial attack of the drug on DNA and the type of cross-linking (either intra- or interstrand cross-links). The 5′ or 3′ direction of intrastrand cross-link formation by the initial monoadduct could be influenced by hydrogen bonding as well. The carrier ligand may also affect biodistribution, rates and type of DNA adduct formation, recognition of damaged DNA by repair enzymes or regulatory/binding proteins, etc. The biological activities of platinum drugs depend on the absolute configuration of the carrier diamine, but the differences are not dramatic in those cases in which the resolved forms were tested.[3,16−24]

One feature of the Pt−DNA adducts that has not drawn much attention is the increased dynamic motion and fluxional character of these adducts. The considerable distortion of the duplex induced in a typical DNA or oligonucleotide by adduct formation most likely leads to large fluxional (breathing) motions. This motion and flexibility have confounded many structural studies (both X-ray and NMR) aimed at assessing the nature of the adduct. For example, we believe that the failure to obtain crystals of the simplest cross-link adduct, *cis*-$Pt(dGpG)_2(NH_3)_2$, may be due to a mixture of conformers resulting from such fluxional motion.[25] Using specially designed carrier ligands, we have recently begun to obtain evidence for many conformers of such cross-linked d(GpG) adducts.[25,26]

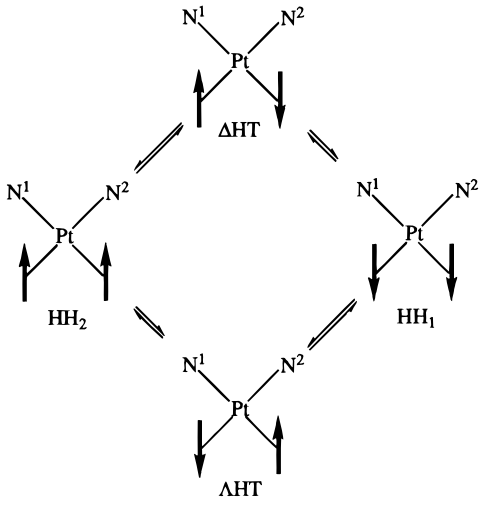

Figure 1. Shorthand representation of ΛHT, ΔHT, and HH conformations with the carrier ligand to the rear. When the carrier is C_2 symmetric and N^1 equals N^2, the two HH forms shown are identical. Arrows represent the **G** bases with **G** H8 near the tip and with the G O6 near the blunt end and projecting toward the carrier. The **G** O6's are used to define HT chirality. When viewing the complexes from the **G** side of the coordination plane, a line connecting the O6 atoms will be rotated (by an angle <90°) clockwise (ΛHT) or counterclockwise (ΔHT) in order to be aligned with the perpendicular to the coordination plane. For the (*S,R*)-**pipen**Pt**G**$_2$ complexes, N^2 and N^1 represent the primary and the secondary amine nitrogens, respectively, and all four (ΛHT, ΔHT, and the two HH) conformations shown are theoretically possible.

Sources of conformational diversity include those typical of DNA (syn vs anti nucleotide residues, N vs S sugar pucker, etc.) and those characteristic of the metal center. Even in the simplest cases, the metal center introduces numerous structural features. For example, neglecting the complications of the backbone and less symmetrical carrier ligands, the cis **G** bases in cross-links can be oriented in a head-to-head (HH) arrangement, in which both H8 atoms lie on the same side of the coordination plane, or in two chiral head-to-tail (HT) arrangements with the H8 atoms on opposite sides of the coordination plane (ΛHT, ΔHT, Figure 1). In addition to the three principal relative base orientations (ΛHT, ΔHT, HH), the cis **G** bases can be tilted in different directions and to different degrees (Chart 2). This tilting and its consequences, as well as the complications of having less symmetrical carrier ligands, will be discussed below. It is thus clear that each orientation has many variants. We will generally specify the conformer only by the relative base orientation, i.e., by the atropisomer (rotamer) designation.

To obtain a better handle on the dynamic and structural properties of the DNA adduct, we must understand the factors that influence the orientational preferences and the dynamic motions involving the metal center. We have been evaluating *cis*-PtA_2**G**$_2$ model complexes, in which A_2 represents two unidentate or one bidentate amine ligand and **G** represents a unidentate guanine ligand. Conformers of these model species have fewer potential variants than adducts with the DNA backbone. The symmetry of the *cis*-PtA_2**G**$_2$ complex influences the number of atropisomers. For C_2-symmetrical A_2 ligands, one HH and two HT atropisomers are possible. With a nonbulky A_2 carrier ligand, interconversion between atropisomers by rotation around the Pt−N7 bonds is fast on the NMR time scale. Usually a single H8 NMR signal is observed, representing an

(16) Kidani, Y.; Inagaki, K.; Iigo, M.; Hoshi, A.; Kuretani, K. *J. Med. Chem.* **1978**, *21*, 1315.
(17) Noji, M.; Okamato, K.; Kidani, Y.; Tashiro, T. *J. Med. Chem.* **1981**, *24*, 508.
(18) Noji, M.; Motoyama, S.; Tashiro, T.; Kidani, Y. *Chem. Pharm. Bull.* **1983**, *31*, 1469.
(19) Coluccia, M.; Correale, M.; Giordano, D.; Mariggiò, M. A.; Moscelli, S.; Fanizzi, F. P.; Natile, G.; Maresca, L. *Inorg. Chim. Acta* **1986**, *123*, 225.
(20) Fanizzi, F. P.; Intini, F. P.; Maresca, L.; Natile, G.; Quaranta, R.; Coluccia, M.; Dibari, L.; Giordano, D.; Mariggiò, M. A. *Inorg. Chim. Acta* **1987**, *137*, 45.
(21) Giannini, G.; Natile, G. *Inorg. Chem.* **1991**, *30*, 2853.
(22) Coluccia, M.; Fanizzi, F. P.; Giannini, G.; Giordano, D.; Intini, F. P.; Lacidogna, G.; Loseto, F.; Mariggiò, M. A.; Nassi, A.; Natile, G. *Anticancer Res.* **1991**, *11*, 281.
(23) Vickery, K.; Bonin, A. M.; Fenton, R. R.; O'Mara, S.; Russell, P. J.; Webster, L. K.; Hambley, T. W. *J. Med. Chem.* **1993**, *36*, 3663.
(24) Fenton, R. R.; Easdale, W. J.; Er, H. M.; O'Mara, S. M.; McKeage, M. J.; Russell, P. J.; Hambley, T. W. *J. Med. Chem.* **1997**, *40*, 1090.
(25) Ano, S. O.; Intini, F. P.; Natile, G.; Marzilli, L. G. *J. Am. Chem. Soc.* **1998**, *120*, 12017.
(26) Ano, S. O.; Intini, F. P.; Natile, G.; Marzilli, L. G. Manuscript in preparation.

Chart 2. Sketches of the ΔHT Atropisomer with Right-Handed and Left-Handed Tilted Variants[a]

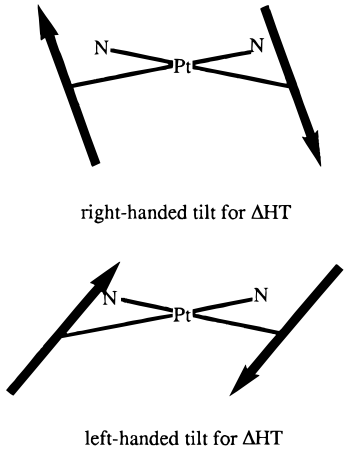

[a] The degree of the tilt is greater when a **G** O6−NH hydrogen bond can be hypothesized.

average signal of all possible guanine orientations.[27−32] Increasing the bulk of the A_2 ligand can slow the Pt−N7 bond rotation so that different atropisomers can be detected by the observation of more than one H8 signal.[7,8,28−30,33−35] However, the HT forms of *cis*-PtA_2**G**$_2$ are favored in almost all cases, and only recently have HH atropisomers in solution been reported.[7,8,35]

We have found that many aspects of Pt drug−DNA interactions can be productively investigated by introducing chiral secondary amine centers into the carrier ligands. To control the chirality of the secondary amines we incorporated adjacent asymmetric carbons with known chirality into the ligand chelate ring. The chiral amine centers are also designed to be close to the DNA in adducts, in contrast to the positioning of chiral groups only at carbon atoms in more traditional carrier ligands. The proximity of the necessarily bulky substituent on the asymmetric nitrogen has the additional advantage that the DNA adducts of Pt complexes of such carrier ligands will have restricted fluxional character. More specifically, our studies with *cis*-PtA_2**G**$_2$ complexes of the carrier ligands **Me$_2$DAB** (*N*,*N*′-dimethyl-2,3-diaminobutane) and **Bip** (2,2′-bipiperidine) (Figure 2) demonstrated that the configuration of the secondary NH's strongly influenced the ΛHT/ΔHT atropisomer ratio such that one or the other HT form was highly favored.[7,8,35,36] We call these diamines chirality-controlling chelate (**CCC**) ligands. (**CCC**)Pt**G**$_2$ complexes with **Me$_2$DAB** and **Bip** carrier **CCC** ligands having the same chirality, e.g., the *S*,*R*,*R*,*S* configurations of the four asymmetric centers (N, C, C, and N) in the chelate ring, and the same **G** derivative have very similar equilibrium atropisomer distributions, chemical shifts, etc. The dynamic properties, however, are very different. The **Bip** derivatives

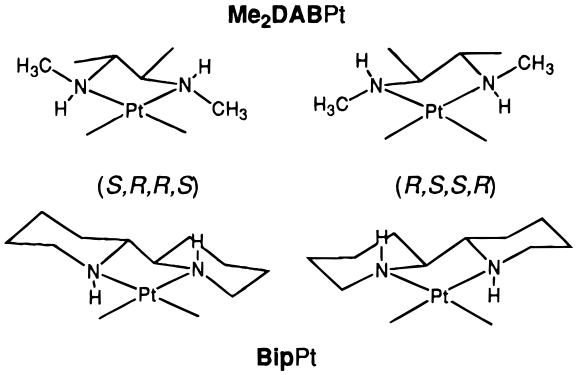

Figure 2. Sketches of **Me$_2$DAB**Pt and **Bip**Pt with *S*,*R*,*R*,*S* and *R*,*S*,*S*,*R* configurations.

atropisomerize very slowly, allowing us to determine the initial distribution of rotamers during the attack of the **G** ligands onto Pt.[35] In contrast, the **Me$_2$DAB** complexes have greater fluxionality, more similar to such behavior in complexes with clinically used carrier ligands. Although the **Me$_2$DAB** complexes have dynamic properties closer to those of the clinical drug, the secondary amine center can isomerize at neutral pH in the **Me$_2$DAB** but not in the **Bip** complexes.

These observations prompted us to study a carrier diamine, 2-aminomethylpiperidine (pipen), which contains a secondary amine resistant to isomerization and a primary amine that could allow some flexibility. This type of complex does have anticancer activity,[37,38] and one-half of it closely resembles clinically used drugs. The piperidine (pip) ring can reduce dynamic motion significantly, and we believe information relevant to clinically used drugs can be obtained by studying these **pipen** complexes since we create an environment very similar to that in clinically used drugs. For *cis*-PtA_2**G**$_2$ complexes with ligands such as **pipen**, which are not C_2-symmetrical, two HH and two HT atropisomers are possible. Although a few studies on dichloro complexes with this kind of carrier ligand are described in the literature,[24,39,40] no report on the adducts of guanine derivatives has appeared.

In this study, racemic **pipen** was prepared and resolved, and complexes of the formula $PtCl_2$(**pipen**) were synthesized and characterized (Figure 3). In these species (with chloride ligands trans to the amine groups), the nitrogen configurations are very stable, and the type and abundance of isomers obtained in a given preparation depend on the experimental conditions used and do not reflect their relative thermodynamic stability. The interaction between 5′-GMP and one of the enantiomers, (*S*,*R*)-$PtCl_2$(**pipen**) (the configurations at the two asymmetric centers are *S* and *R* at N and C, respectively), was studied by NMR and CD techniques.

Experimental Section

Synthesis of 2-Aminomethylpiperidine (Pipen). 2-Aminomethylpyridine (10 g, 0.092 mol) in ethanol (700 mL) was hydrogenated using sodium metal (45 g). The reaction temperature was kept initially at 50 °C, and as the reaction proceeded and the medium became viscous, the temperature was increased until refluxing occurred. After ∼2 h, the reaction mixture was cooled to room temperature and brought to

(27) Li, D.; Bose, R. N. *J. Chem. Soc., Dalton Trans.* **1994**, 3717.
(28) Cramer, R. E.; Dahlstrom, P. L. *J. Am. Chem. Soc.* **1979**, *101*, 3679.
(29) Cramer, R. E.; Dahlstrom, P. L.; Seu, M. J. T.; Norton, T.; Kashiwagi, M. *Inorg. Chem.* **1980**, *19*, 148.
(30) Cramer, R. E.; Dahlstrom, P. L. *Inorg. Chem.* **1985**, *24*, 3420.
(31) Ano, S. O.; Kuklenyik, Z.; Marzilli, L. G. In *Cisplatin: Chemistry and Biochemistry of a Leading Anticancer Drug*; Lippert, B., Ed.; VHCH-Wiley-VCH: Basel, in press.
(32) Inagaki, K.; Dijt, F. J.; Lempers, E. L. M.; Reedijk, J. *Inorg. Chem.* **1988**, *27*, 382.
(33) Miller, S. K.; Marzilli, L. G. *Inorg. Chem.* **1985**, *24*, 2421.
(34) Reily, M. D.; Marzilli, L. G. *J. Am. Chem. Soc.* **1986**, *108*, 6785.
(35) Ano, S. O.; Intini, F. P.; Natile, G.; Marzilli, L. G. *J. Am. Chem. Soc.* **1997**, *119*, 8570.
(36) Marzilli, L. G.; Intini, F. P.; Kiser, D.; Wong, H. C.; Ano, S. O.; Marzilli, P. A.; Natile, G. *Inorg. Chem.* **1998**, *37*, 6898.
(37) Morikawa, K.; Honda, M.; Endoh, K.; Matsumoto, T.; Akamatsu, K.; Mitsui, H.; Koizumi, M. *J. Pharm. Sci.* **1990**, *79*, 750.
(38) Tanabe Seiyaku Co., Ltd. Jpn. Kokai Tokkyo Koho JP 59 67,262, 1984.
(39) Saito, R.; Goto, M.; Hirose, J.; Kidani, Y. *Bull. Chem. Soc. Jpn.* **1992**, *65*, 1428.
(40) Saito, R.; Goto, M.; Hirose, J.; Kidani, Y. *Bull. Chem. Soc. Jpn.* **1992**, *65*, 2118.

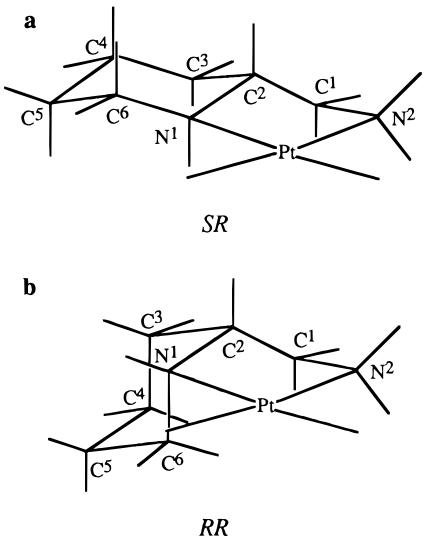

Figure 3. For a given configuration (*R*) of C^2 of the free amine ligand, there are two possible complexed ligand configurations of the N^1-coordinated nitrogen: (**a**) *S* and (**b**) *R*.

pH 2 with concentrated hydrochloric acid, the solution was filtered (to remove NaCl), and the solvent was evaporated at reduced pressure. The residue was dissolved in water (20 mL), and after the addition of an excess of potassium hydroxide, the solution was extracted five times with 100 mL of diethyl ether. The ether was removed under reduced pressure and the residue distilled (at 35 °C, 7 mmHg pressure), yielding 5−6 g of a mixture of **pipen** and 2-aminomethylpyridine as a colorless, oily liquid. Separation of this mixture was achieved by taking advantage of the different rates of crystallization of their hydrochloride salts from ethanol. Whereas the salt of 2-aminomethylpyridine precipitated immediately, the **pipen** salt precipitated only after the solution was kept at 0 °C for 24 h; yield: 4.5 g (0.024 mol, 26%) of pure **pipen**.

The **pipen** purity was monitored using NMR and GC mass spectrometry. The gas chromatogram obtained showed only one peak, and the corresponding mass spectrum could be attributed to **pipen** from peaks at *m*/*z* 84 ($C_5H_{10}N$) and 114 ($C_6H_{14}N_2$).

Resolution of *rac*-Pipen. Addition of a solution of dibenzoyl-(+)-tartaric acid (DBTA, 6.5 g) in absolute ethanol to a solution of racemic **pipen** (2.0 g) in diethyl ether gave a precipitate, which was recrystallized several times from water/ethanol (20:80 v/v). The enrichment of a given sample in one enantiomeric form was monitored by HPLC (chiral column DAC-DNB, eluant hexane/dichloromethane, 7:3 v/v) by converting the DBTA salt to the free diamine (by dissolving it in the minimum amount of water, treatment with an excess of KOH, and extraction into diethyl ether) and then making the amide derivative using trifluoroacetic anhydride. The derivative of the racemic form had previously been studied and the retention times noted. This procedure was repeated during each stage of recrystallization until only one enantiomeric form was observed in the HPLC trace. The GC−MS spectrum of the trifluoroacetamide derivative showed a single peak in the gas chromatogram at 306 *m*/*z*. Next the derivative was converted to the hydrochloride salt (diethyl ether extracts of the free amine were saturated with HCl gas) and characterized by elemental analysis, ^{1}H NMR spectroscopy, and the $[\alpha]_D$ measured as −2.54° (1% solution in methanol).

After the DBTA salt of one enantiomer was removed, the other enantiomer could be isolated from the mother liquor by evaporating the solvent, treating the oily residue with potassium hydroxide, and extracting the free amine with diethyl ether. Treatment of the ether solution with hydrogen chloride gas afforded a precipitate of the amine hydrochloride, which was recrystallized from ethanol. The $[\alpha]_D$ measurement (1% in methanol) gave the same value, but with opposite sign, as that of the amine hydrochloride obtained from the DBTA salt. The latter enantiomer was also isolated from the racemic mixture using dibenzoyl-(−)-tartaric acid as the resolving agent.

Determination of the Absolute Configuration. For the free **pipen** enantiomers with $[\alpha]_D$ of −19° and +19° (2% in ethanol), the absolute configuration at the chiral carbon has been determined to be *R* and *S*, respectively.[41] We have checked that an $[\alpha]_D$ of +2.54° (1% in methanol) for the hydrochloride corresponds to an $[\alpha]_D$ of ca. −15° (2% in ethanol) for the free amine.

Preparation of Dichloro(pipen)platinum(II) Isomers. When dimethyl sulfoxide (DMSO) (2 mmol, 0.142 mL) was added to a stirred aqueous solution of $K_2[PtCl_4]$ (1 mmol, 0.415 g) in water (20 mL) maintained at 70 °C, the solution became yellow as $PtCl_2(DMSO)_2$ formed in situ. An aqueous solution of **pipen** hydrochloride (1 mmol), neutralized with LiOH (2 mmol), was added slowly to the solution of $PtCl_2(DMSO)_2$. The mixture was stirred at 95 °C for 1 h. The yellow precipitate that formed was collected by filtration, washed with water and diethyl ether, and dried. Yields in all cases were >80%. Elemental analyses of the $PtCl_2$(**pipen**) complexes are given in the Supporting Information.

Preparation of Dinitrato(pipen)platinum(II). A suspension of $PtCl_2$(**pipen**) (1 mmol, 0.380 g) in acetone (40 mL), stirred at room temperature, was treated with a solution of $AgNO_3$ (2 mmol, 0.338 g) in a minimum of water. The solution was left to stir for 2 h, during which time the yellow color of the $PtCl_2$(**pipen**) disappeared and a white precipitate of AgCl formed. The solution was filtered and evaporated under reduced pressure to afford a quantitative yield (0.455 g) of $Pt(NO_3)_2$(**pipen**) as a colorless crystalline powder.

Preparation of (*S*,*R*)-PipenPt(5′-GMP)$_2$ Solutions. The pH of a solution of 5′-GMP (20 mM, Sigma, used as received) in D_2O (0.6 mL) was adjusted to ∼3.5. (*S*,*R*)-$PtCl_2$(**pipen**) (0.5 equiv) was then added, the pH of the reaction mixture adjusted back to ∼3.5, and the mixture stirred at 50 °C for 3 days.

NMR Spectroscopy. ^{1}H NMR 1D spectra were obtained with either a GE GN 500 MHz or a GE Omega 600 MHz spectrometer. For pH titration experiments, 3-(trimethylsilyl)tetradeuterosodium propionate (TSP) was used as an external reference; otherwise, all spectra were referenced to the HOD peak. The 2D phase-sensitive NOESY/EXSY,[42] 600 MHz spectra (1K × 2K matrix, 300 ms mixing time, 32 acquisitions per t_1) were obtained at 5 °C with a spectral window in both dimensions of 6250 Hz. Spectra were processed with the FELIX program (Molecular Simulations, Inc.). A 1 Hz exponential multiplication factor was applied in the acquisition dimension. The evolution dimension was zero filled to 2K points, and a 90° shifted skewed sine squared function was applied.

$^{31}P\{^1H\}$ NMR spectra recorded on the 600 MHz spectrometer were referenced to trimethyl phosphate (TMP). The pK_a of each phosphate group (in 90% H_2O/10% D_2O with NaCl added to give an ionic strength of 0.1 M) was determined by curve fitting the following equation: $\delta = (\delta_A[H^+] + \delta_B K_a)/([H^+] + K_a)$, where the ^{31}P chemical shift of a given phosphate group is δ at a given pH, δ_A when protonated, and δ_B when deprotonated. The pH (uncorrected) of samples in NMR tubes was adjusted with 1% and 10% (w/v) D_2O solutions of DNO_3 or NaOD.

Circular Dichroism (CD) Spectroscopy. CD spectra of ∼4×10^{-5} M solutions were recorded on a JASCO 600 spectropolarimeter at ambient temperature. To improve signal/noise, four spectra were acquired in succession and averaged.

Results

Synthetic Methods. The syntheses of **pipen** and of the corresponding Pt complexes have been reported;[37] however, we used a simpler, more convenient procedure here. Furthermore, we separated the two enantiomeric forms of the free ligand and synthesized the Pt complexes as single, pure stereoisomers. Hydrogenation of the 2-aminomethylpyridine was effected with sodium metal in ethanol. The yield was comparable to, if not better than, that obtained by reduction with hydrogen gas in the presence of PtO_2 as catalyst.[37] Our procedure leads to a crude product containing unchanged 2-aminomethylpyridine as the main impurity. Purification of the amine proved straightforward,

(41) Hardtmann, G. E.; Houlihan, W. J.; Giger, R. K. A. (Sandoz-Patent-GmbH). Ger. Offen. DE 3,702,943, 1987.
(42) Kumar, A.; Ernst, R. R.; Wüthrich, K. *Biochem. Biophys. Res. Commun.* **1980**, *95*, 1.

Table 1. Proton Chemical Shifts (ppm) for **Pipen**·2HCl and $[Pt(D_2O)_2$**pipen**$)]^{2+}$ in D_2O

	C^1H_2	C^2H	C^6H_2	C^5H_2	C^4H_2	C^3H_2
ligand	3.20	3.40	3.40	1.75	1.90	1.75
			2.90	1.50	1.50	1.50
complex	2.30	2.70	2.95	1.45	1.80	1.70
	2.25		2.70		1.20	1.45

however, by our taking advantage of the different rates of precipitation of the amine hydrochlorides from ethanol. In the resolution of the enantiomers carried out in the classical way with DBTA as resolving agent, solvent composition (water/ethanol, ~20:80 v/v) was critical for effecting a quantitative separation of the two enantiomers after only two or three subsequent crystallizations.

Our $PtCl_2$(**pipen**) preparative procedure required only a stoichiometric amount of the free ligand, which was added to a reactive neutral substrate, $PtCl_2(DMSO)_2$. The latter was prepared in situ by the aqueous reaction of $K_2[PtCl_4]$ and DMSO (1:2 molar ratio). Two $PtCl_2$(**pipen**) isomers could be formed from a pure **pipen** enantiomer (e.g., having the *R* configuration at the asymmetric carbon), since, upon coordination to platinum, the configuration at the secondary nitrogen becomes a resolvable chiral center (Figure 3). However, as already observed in other cases, the configuration of the carbon is likely to influence the configuration on the adjacent nitrogen. This is particularly true for a complex like the one under investigation, in which the two chiral centers (C^2 and N^1) are linked not only by a direct bond but also through the six- and five-membered rings. Of the two possible $PtCl_2$(**pipen**) isomers, only one isomer was formed in quantitative yield.

^{1}H NMR Spectrum of Pipen Dihydrochloride. The ^{1}H NMR spectrum of **pipen**·2HCl in D_2O at pH 6.5 was complicated, and it was necessary to perform a COSY experiment in order to assign the peaks (integrations are given in italics in parentheses). The downfield multiplets (2.8−3.4 ppm, *five*) were presumed to be from CH's next to the nitrogens (C^1H_2, C^2H, and C^6H_2). The upfield multiplets (1.3−2.0 ppm, *six*) were assumed to be from the other CH's (C^3H_2, C^4H_2, and C^5H_2). From the COSY spectrum (Supporting Information), the multiplet centered at 3.2 ppm (*two*) was assigned to C^1H_2, as these protons were strongly coupled, and there was no evidence of coupling with upfield multiplets. These protons are expected to couple only with C^2H; thus the signal of the latter proton must be in the multiplet at 3.4 ppm (*two*). This multiplet must also contain one of the C^6H_2 signals. The other C^6H_2 signal must be that of the multiplet centered at 2.9 ppm (*one*), which has a strong cross-peak with the multiplet at 3.4 ppm. (See Table 1.)

Assignments of the multiplets between 1.3 and 2.0 ppm begin with the C^6H multiplet (at 2.9 ppm), which can have cross-peaks only with the C^5H_2 signals; thus the C^5H_2 signals must be part of the multiplets centered at 1.75 (*two*) and at 1.5 ppm (*three*). On the other hand, the C^2H multiplet (at 3.4 ppm) can have cross-peaks only with C^3H_2 in the high-field region; therefore the C^3H_2 signals must also be part of the multiplets centered at 1.75 and 1.5 ppm (the strong cross-peaks between the multiplets at 1.75 and 1.5 ppm are in accord with each multiplet containing one of the signals of the geminal protons bound to C^3 and to C^5). Finally, the C^4H_2 signals must be the multiplet centered at 1.9 (*one*) and part of the multiplet at 1.5 ppm (there is a strong cross-peak between these multiplets). As expected, the multiplet centered at 1.9 ppm has no coupling with signals in the low-field region.

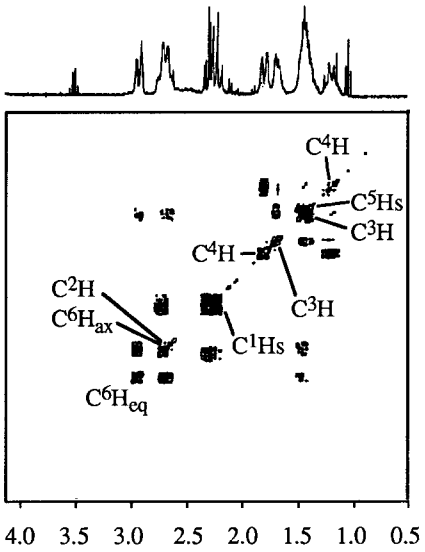

Figure 4. COSY spectrum of $[Pt(D_2O)_2$(**pipen**$)]^{2+}$ in D_2O.

$[Pt(H_2O)_2$(pipen)$]^{2+}$. The insolubility of the $PtCl_2$(**pipen**) complexes in most organic solvents and in water limited our studies. Therefore, $PtCl_2$(**pipen**) was converted into the dinitrato complex, which forms the diaqua complex in water. The COSY spectrum (Figure 4) of 5 mM $Pt(NO_3)_2$(**pipen**) in H_2O at pH 6.5 was analyzed as above. The low-field region contained three multiplets (at 2.95, 2.7, and 2.3 ppm). This last multiplet consists of a doublet of doublets at 2.3 ppm and a pseudotriplet at 2.25 ppm. The doublet of doublets is assigned to C^1H_{eq}, which can have only one strong coupling (with the geminal C^1H_{ax}), while the pseudotriplet is assigned to C^1H_{ax}, which can have two strong couplings (with the geminal C^1H_{eq} and with C^2H_{ax}). The multiplets at 2.3 and 2.25 ppm have cross-peaks with the multiplet at 2.7 ppm (which therefore must contain the signal of C^2H), but not with the multiplets in the 1.1−1.9 ppm region. The peak centered at 2.95 ppm (*one*) is assigned to C^6H_{eq}, which is expected to have only one strong coupling (with the geminal C^6H_{ax}). The C^6H_{ax} signal, which falls in the multiplet at 2.7 ppm overlapping with C^2H, is also strongly coupled with C^5H_{ax}.

The remaining multiplets are assigned to the more shielded pip ring protons. The C^6H_2 signals have cross-peaks only with the broad multiplet centered at 1.45 ppm (*three*), which thus must contain both C^5H_2 signals. The one-proton multiplets at 1.8 and 1.2 ppm have a strong cross-peak with each other but not with the low-field multiplets; therefore, they are assigned to C^4H_2. The multiplet at 1.7 ppm (*one*), which has a strong cross-peak with the multiplet at 1.45 ppm, is assigned to one C^3H_2 signal. The other C^3H_2 signal is the third signal in the multiplet at 1.45 ppm, an assignment supported by the cross-peak between the multiplet at 1.45 ppm and the multiplet at 2.7 ppm already assigned to the C^2H signal. C^2H (which is axial) is expected to have strong coupling with only the axial C^3H; therefore the C^3H_{ax} and the C^3H_{eq} signals are at 1.45 and 1.7 ppm, respectively.

To determine the configuration of the N^1 atom of the coordinated **pipen** ligand (**a** or **b** in Figure 3), $[Pt(H_2O)_2$-(**pipen**$)]^{2+}$ was converted to the dimethylmalonato (Me_2mal) derivative in the NMR tube in D_2O at pH 7. The Me_2mal ligand is a good probe of diamine stereochemistry since one Me group projects above and the other below the Pt coordination plane. In the case of the C_2-symmetric **Bip**Pt(Me_2mal), where the pip rings lie close to the coordination plane such as shown for **a** (Figure 3), the Me signal is at 1.82 ppm. As expected, the non-C_2-symmetric **pipen**Pt(Me_2mal) has two Me signals, and the

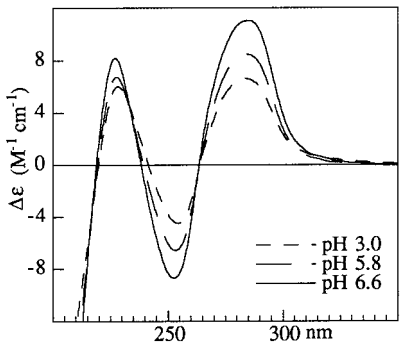

Figure 5. CD spectrum of (*S,R*)-**pipen**Pt(5′-GMP)$_2$ below pH 7.

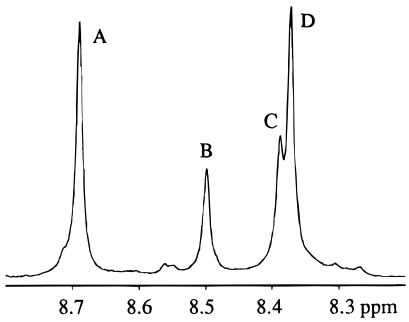

Figure 6. H8 region of the NMR spectrum of (*S,R*)-**pipen**Pt(5′-GMP)$_2$ at pH 3.

signals fall at nearly the same shift (1.78 and 1.80 ppm) and close to that of the **Bip** analogue. Thus the configuration of the rings must be similar in both compounds, and we conclude that **pipen** has the **a** stereochemistry (Figure 3). Furthermore, when the pH was then brought to 10.5, where base-catalyzed isomerization at N^1 can occur, two new Me signals of equal intensity appeared at 1.64 and 1.98 ppm. The ratio between the initial and the new pair of signals was ~2:1. Beyond any reasonable doubt, the new pair of signals is due to the formation of an isomer in which the pip ring projects out of the plane such as shown in Figure 3b; in this isomer, the C and N atoms have equal configurations (*R,R*).

We conclude that the starting compounds used in this study (with the exception of the new isomer just mentioned) contain (*S,R*)-**pipen**. This conclusion is supported by our finding that the CD spectrum of the pH 4.2 aqueous solution of (*S,R*)-Pt(NO_3)$_2$(**pipen**) (Supporting Information) has positive peaks at 370 and 272 nm and a negative peak at 240 nm. For the peak at 270 nm, assigned to the $^1A_1 \rightarrow {}^1A_2$ transition in analogous compounds,[43] $\Delta\epsilon = 0.35\ M^{-1}\ cm^{-1}$. Although the peaks are at shorter wavelengths, the shape of the spectrum below 300 nm is very similar to all reported spectra of (*N*-alkyl-1,2-alkanediamine)$PtCl_2$ complexes with the configuration at the amine N center shown in Figure 3a. The positive and negative peaks at 303 and 267 nm, respectively, in these spectra[39,40] and the positive and negative peaks at 272 and 240 nm, respectively, in the CD spectrum of (*S,R*)-Pt(NO_3)$_2$(**pipen**) are consistent with all the other evidence that the configuration of N^1 in **pipen** is *S*.

(*S,R*)-PipenPt(5′-GMP)$_2$. The CD spectrum of (*S,R*)-**pipen**Pt(5′-GMP)$_2$ at pH 3 (Figure 5) shows positive peaks at about 285 and 230 nm and negative peaks at 250 and 205 nm. This spectrum is similar to the characteristic spectra of (*S,R,R,S*)-**Me$_2$DAB**Pt**G**$_2$, in which the major conformation is ΛHT, as determined by 2D NMR experiments.[36]

In the ^{1}H NMR spectrum of (*S,R*)-**pipen**Pt(5′-GMP)$_2$ at pH 3, four H8 peaks (A−D) comprise >90% of the H8 intensity in the 8.3−8.7 ppm region (Figure 6). The downfield shift of the H8 signals compared to this signal for free 5′-GMP and the acidic pH used for sample preparation indicate that 5′-GMP is coordinated via N7. By integration, the areas of peaks A and D are equivalent and the areas of peaks B and C are equivalent. The ratio of the sum of the areas of A and D to that of B and C is 7:3. The 1.0−3.1 ppm region contains the methylene and the methine signals of the **pipen** moiety. The 5.5−6.2 ppm region contains five NH signals; these have cross-peaks to the methylene and the methine signals.

In the 2D NOESY spectrum, the absence of any NOE cross-peaks between these H8 signals (Supporting Information) indicates that the major atropisomers are head-to-tail (HT). Otherwise, NOE cross-peaks would be observed due to the proximity of H8 protons in the head-to-head (HH) form. Importantly, there are no EXSY cross-peaks between the H8 signals, indicating that the dynamic equilibrium between the HT forms (Figure 1) is extremely slow.[7,8,27,35,36,44,45]

Table 2. (*S,R*)-**Pipen**Pt(5′-GMP)$_2$ **G** H8 Chemical Shifts (ppm) and Cross-Peaks[a] with NH and C^6H Signals[b,c]

H8	shift	NH	C^6H'	C^6H''	H_1'
A	8.69	N^1H: 6.16 (8.6)	2.39 (15)	2.72 (1.4)	5.88
B	8.49	N^2Hs: 5.78 (2.9)			5.88
C	8.38	N^1H: 5.56 (0)	2.52 (2.7)	2.89 (2.9)	5.79
D	8.35	N^2H': 5.61 (4.9)			5.69
		N^2H'': 5.84 (5.5)			

[a] Relative volumes of the cross-peaks are listed in parentheses. [b] At pH 3 and 5 °C. [c] Also included are the **G** H_1' chemical shifts.

The H8 signals have NOE cross-peaks to the NH and C^6H signals (Table 2 and Supporting Information). We shall discuss first the interpretation of peaks A and D for the most abundant species and then peaks B and C. For the initial discussion, we exclude the possibility that signals A and D arise from more than one atropisomer. The cross-peak pattern, peak A to one NH signal (at 6.16 ppm) and peak D to two NH signals (at 5.61 and 5.84 ppm), demonstrates that $\mathbf{G_A}$ is cis to the secondary amine and $\mathbf{G_D}$ is cis to the primary amine. Further confirming that $\mathbf{G_A}$ is cis to the secondary amine, peak A has cross-peaks with the C^6H' and C^6H'' signals at 2.39 and 2.72 ppm, respectively. (H′ and H″ designate upper- and lower-field CH_2 signals, respectively.)

From the NOE cross-peaks between NH and CH_2 and CH signals within the **pipen** ligand (Figure 7, Table 3), the relative positions of the protons can be determined. From the cross-peaks, we can also determine if NH_2 and CH_2 protons are axial or equatorial, H_{ax} and H_{eq}, respectively. The relatively small N^1H-C^2H NOE cross-peak indicates that N^1H is in the axial position, which is possible only if the secondary amine nitrogen and C^2 have different chirality (Figure 3). (Thus the conclusion drawn on the basis of ^{1}H NMR analysis of the Me_2mal complex is confirmed.) N^1H has a smaller NOE cross-peak with the C^6H'' signal than with the C^6H' signal, indicating that C^6H' is C^6H_{eq} while C^6H'' is C^6H_{ax}. The C^2H-N^2H' cross-peak is weaker than the C^2H-N^2H'' cross-peak, indicating that N^2H' is N^2H_{eq} and N^2H'' is N^2H_{ax}. Finally, the $C^1H'-N^2H'$ cross-peak is stronger than the $C^1H'-N^2H''$ cross-peak, indicating that C^1H' is C^1H_{ax}. The $C^1H''-N^2H'$ and $C^1H''-N^2H''$ cross-peaks are comparable, indicating that C^1H'' is C^1H_{eq}. N^1H has an NOE cross-peak with

(43) Ito, H.; Fujita, J.; Saito, K. *Bull. Chem. Soc. Jpn.* **1967**, *40*, 2584.
(44) Li, D.; Bose, R. N. *J. Chem. Soc., Chem. Commun.* **1992**, 1596.
(45) Williams, K. M.; Cerasino, L.; Intini, F. P.; Natile, G.; Marzilli, L. G. *Inorg. Chem.* **1998**, *37*, 5260.

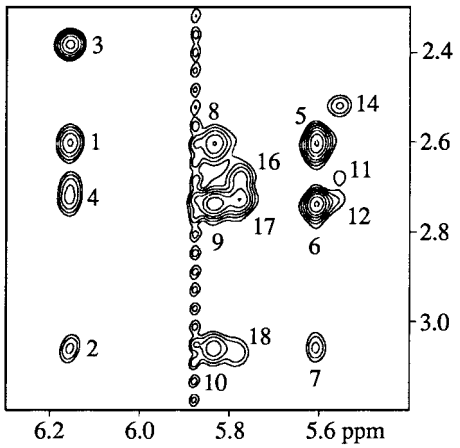

Figure 7. NOE cross-peaks between NH and methylene and methine proton signals of (*S,R*)-**pipen**Pt(5′-GMP)$_2$. Peaks are numbered according to the assignments in Table 3. At this contour level, cross-peaks 13 and 15 cannot be observed.

Table 3. Chemical Shifts and Relative Volumes of NH−CH NOE Cross-Peaks within the **Pipen** Moiety of (*S,R*)-**Pipen**Pt(5′-GMP)$_2$

Major Atropisomer

peak	N^1H	N^2H'	N^2H''	C^1H'	C^1H''	C^2H	C^6H'	C^6H''	rel vol
1	6.16			2.60					41.6
2	6.16					3.06			7.8
3	6.16						2.39		64.0
4	6.16							2.72	22.5
5		5.61		2.60					94.4
6		5.61			2.74				191.0
7		5.61				3.06			6.2
8			5.84	2.60					42.7
9			5.84		2.74				247.2
10			5.84			3.06			31.5

Minor Atropisomer

peak	N^1H	N^2H	C^1H'	C^1H''	C^2H	C^6H'	C^6H''	rel vol
11	5.56		2.68					7.5
12	5.56			2.73				*a*
13	5.56				3.06			2.8
14	5.56					2.52		10.0
15	5.56						2.89	1.0
16		5.78	2.68					7.2
17		5.78		2.73				85.3
18		5.78			3.06			6.2

[a] Cannot be determined due to overlap of signal.

C^1H', which is only possible if N^1H is in the axial position (Figure 3). This further demonstrates that N^1 and C^2 have opposite configurations.

To determine whether the most abundant HT conformer was Δ or Λ, we estimated the distance of H8 with respect to the two axial protons, N^1H and C^6H_{ax}, which are on opposite sides of the platinum coordination plane. The strong A−N^1H and weak A−C^6H_{ax} NOE cross-peaks (Table 2) indicate that $\mathbf{G_A}$ H8 lies below the Pt coordination plane. The D−N^2H'' NOE cross-peak is stronger than the D−N^2H' cross-peak, indicating that $\mathbf{G_D}$ H8 lies above the Pt coordination plane. These results demonstrate that the most abundant species is ΛHT (Figure 1).

For the second most abundant species (Table 2), the B−N^2H NOE cross-peak at 5.78 ppm indicates that $\mathbf{G_B}$ is cis to the primary amine. The C−C^6H' and C−C^6H'' cross-peaks indicate that $\mathbf{G_C}$ is cis to the secondary amine. The relative positions of the protons in the **pipen** moiety for this atropisomer can be deduced as described above (Table 3). The results are as follows: C^6H' is C^6H_{eq}; C^6H'' is C^6H_{ax}; C^1H' is C^1H_{ax}; and C^1H'' is C^1H_{eq}.

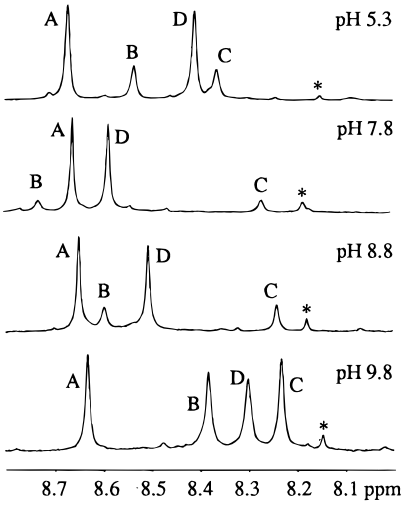

Figure 8. H8 region of the ^{1}H NMR spectra of (*S,R*)-**pipen**Pt(5′-GMP)$_2$ at various pH values; (∗) free 5′-GMP.

Because of the overlap of the N^2H signals, the orientation of $\mathbf{G_B}$ cannot be determined. Peak C has a cross-peak with the C^6H signal but none with the N^1H signal, indicating that this H8 lies above the Pt coordination plane. The absence of an NOE between peaks B and C strongly suggests that this atropisomer is ΔHT.

pH Titration by ^{31}P NMR. At pH 3.7, the major ΛHT atropisomer had signals at 0.21 and 0.29 ppm that shifted to 3.79 and 3.81 ppm, respectively, as the pH was raised to 8.1. The minor ΔHT atropisomer had signals at 0.34 and 0.36 ppm at pH 3.7, which shifted downfield and overlapped at 3.72 ppm at pH 8.1. The presence of four ^{31}P signals allowed us to determine the pK_a values of each phosphate group. The pK_a values were determined to be 5.81 and 5.84 for the major HT conformer and 5.86 and 6.13 for the minor HT conformer. The pK_a of unplatinated 5′-GMP was determined to be 6.23 in a separate experiment.[45] Thus, except for one phosphate group, platination caused the pK_a values to decrease by ∼0.4 unit. However, we did not determine whether this phosphate group with 0.1 unit pK_a drop was in $\mathbf{G_B}$ or $\mathbf{G_C}$.

pH Titration by ^{1}H NMR. ^{1}H NMR spectral changes from pH 5.3 to 7.8 (Figure 8) demonstrated that the major ΛHT atropisomer became highly favored on phosphate group deprotonation. Deprotonation of the **G** N1H's at higher pH reversed this trend and by pH 9.8 the ΔHT form became the major conformer (Figure 8). During the pH titration, the B and D H8 signals for the **G**'s cis to the primary amine of the ΔHT and ΛHT atropisomers, respectively, experienced large shift changes compared to signals A and C.

pH Titration by CD. Raising the pH of the (*S,R*)-**pipen**Pt(5′-GMP)$_2$ solution from 3.0 to 6.6 increased the CD signal intensities (Figure 5). This result is consistent with the NMR data showing that phosphate group deprotonation favored the ΛHT atropisomer. Further increases in pH caused decreases in signal intensities; at pH 9.9, the CD signal started to invert (Figure 9), consistent with the NMR data demonstrating that the ΔHT atropisomer was favored at high pH. The agreement between the CD and the NMR studies strongly suggests that the signs of the CD features can be used to determine the conformation of the major atropisomer.

pH Jump. NMR and CD pH titration results are correlated with the assumption that the ΛHT and ΔHT atropisomers have similar CD signal intensities but with opposite sign. If the assumption is correct, the resultant CD spectrum of a mixture

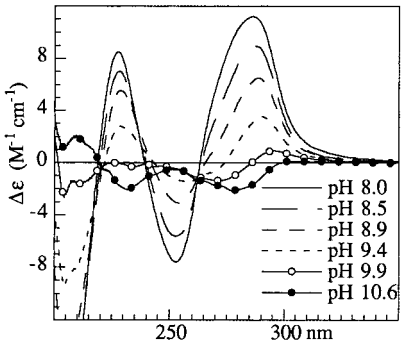

Figure 9. CD spectra of (*S*,*R*)-**pipen**Pt(5′-GMP)$_2$ above pH 7.

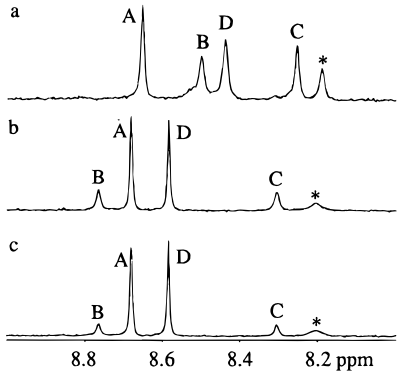

Figure 10. H8 region of the ^{1}H NMR spectrum of (*S*,*R*)-**pipen**Pt(5′-GMP)$_2$ (a) at pH 9.5 and at pH 6.9, recorded (b) 3 min and (c) 30 min after pH adjustment; (∗) free 5′-GMP.

provides information about the conformation of the dominant rotamer. Since the two atropisomers are not true mirror images of each other, the above assumption had to be tested. Furthermore, there is the problem that the CD signal reflects both rotamer redistribution and the pH dependence of the CD signals. Thus, although CD signal intensities changed in the manner expected from changes in NMR signals, we designed "pH jump experiments" to eliminate uncertainties from any pH effect. The pH of an (*S*,*R*)-**pipen**Pt(5′-GMP)$_2$ solution was left at 9.5 for 1 h; enough acid was added to drop the pH to slightly less than neutral, and immediately the solution was examined over time. Separate such experiments were performed for NMR and CD measurements. Fortunately, the rate of the atropisomer redistribution was slow enough ($t_{1/2} \sim 3$ min) that we could easily monitor the time-dependent spectral changes.

From the pH jump NMR spectra, the abundance of the dominant atropisomer increased in 3 min from 58% at pH 9.5 to 72% at pH 6.9 (Figure 10). The final abundance (83%) was consistent with the pH titration results obtained slowly and discussed above (Figure 8). The first spectrum recorded in the pH jump CD studies (Figure 11) showed an increase in signal intensity, as well as a clear shift of the signal maxima and minima toward shorter wavelengths and distinct changes in the signal shape. With time, the signal intensity eventually reached about twice the pH 9.5 value. Spectra obtained in both types of measurements when the pH was returned to near neutral revealed that no irreversible processes had occurred. These experiments clearly demonstrate a correlation between the CD signal intensity and the population of the major isomer.

Discussion

Previously, we studied (**CCC**)Pt**G**$_2$ complexes with two chiral N centers (Figure 2). Our studies established the empirical principle that the chirality of the C_2-symmetrical **CCC** ligands

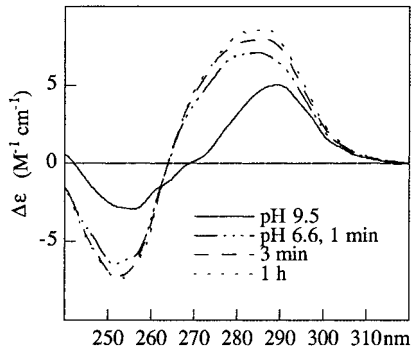

Figure 11. CD spectra of (*S*,*R*)-**pipen**Pt(5′-GMP)$_2$ at pH 9.5 and at different times after the pH was adjusted to 6.6.

determined the chirality of the dominant HT conformer at pH 7 and below; the nature of the **G** N9 substituent had only a modulating effect on the atropisomer distribution.[7,35,36] The dominant HT form had both **G** O6's on the opposite side from the NH group even for (**CCC**)Pt**G**$_2$ complexes with a simple G such as 9-ethylguanine, which has no hydrogen-bonding groups in the N9 substituent. Therefore hydrogen bonding involving **G** O6 (Chart 1) can have at best a secondary effect on distribution. Even the presence of phosphate groups on the N9 substituent does not override this preference, especially at low pH, where the phosphate group is protonated.

In this study of (*S*,*R*)-**pipen**Pt(5′-GMP)$_2$, the carrier ligand has only one chiral N center; therefore, attenuation of the degree of stereochemical control would be expected. For both (*S*,*R*,*R*,*S*)-**Me$_2$DAB**Pt(5′-GMP)$_2$ and (*S*,*R*,*R*,*S*)-**Bip**Pt(5′-GMP)$_2$, the ΛHT:ΔHT ratio determined by NMR methods is >6:1 at pH 3.[35,36] For (*S*,*R*)-**pipen**Pt(5′-GMP)$_2$, this ratio is 7:3 at pH 3, consistent with the decreased stereocontrol expected. In both previously studied systems and in (*S*,*R*)-**pipen**Pt(5′-GMP)$_2$ (see below), the rare HH forms are minor species; the HH form has weak CD signals.[35] The CD spectrum is dominated by HT forms.[35] The CD spectrum of (*S*,*R*)-**pipen**Pt(5′-GMP)$_2$ is similar to those found in other cases of ΛHT dominance, (*S*,*R*,*R*,*S*)-**Me$_2$DAB**Pt-(5′-GMP)$_2$[36] and (*S*,*R*,*R*,*S*)-**Bip**Pt(5′-GMP)$_2$.[35] This result suggests that the *S* configuration of only one secondary amine nitrogen can favor the ΛHT atropisomer. Furthermore, it lends further support to the empirical principle that the absolute configuration of secondary amines of the **CCC** ligands controls which chiral HT isomer is favored.

One of our goals was to determine the factors underlying the empirical principle. In particular, we wished to assess how potential hydrogen-bonding interactions, possible steric interactions, and any internucleotide interactions influence the relative stability of the atropisomers. A previous study employing complexes with non-C_2-symmetrical carrier ligands, (*S*,*R*,*R*,*R*)-**Me$_2$DAB**Pt(5′-GMP)$_2$ and (*S*,*S*,*S*,*R*)-**Me$_2$DAB**Pt(5′-GMP)$_2$,[8] revealed no clear single factor to account for stereocontrol. Although the **pipen** carrier ligand is also non C_2 symmetric, dynamic motions are less pronounced than for the **Me$_2$DAB** complexes. The stability of the secondary amine to isomerization at high pH allows for a more extensive study.

In the ^{1}H NMR spectrum of (*S*,*R*)-**pipen**Pt(5′-GMP)$_2$ at low pH, the secondary amine N^{1}H signal of the ΛHT form has the most downfield chemical shift (6.16 ppm) of the NH signals for this complex. In the ΛHT conformation, the phosphate group of the 5′-GMP cis to the secondary amine is on the same side of the coordination plane as the N^1 proton (Chart 3; the tilting of the **G** bases depicted in this chart is discussed below). Therefore, the downfield shift most probably is caused by the phosphate group, either by its hydrogen bonding to NH (Chart

Chart 3. Relationship of the Structure of the (*S*,*R*)-**Pipen**Pt Moiety to the Schematic Representation of the Moiety in Depictions of the ΛHT and ΔHT Atropisomers of (*S*,*R*)-**Pipen**Pt(5′-GMP)$_2$[a]

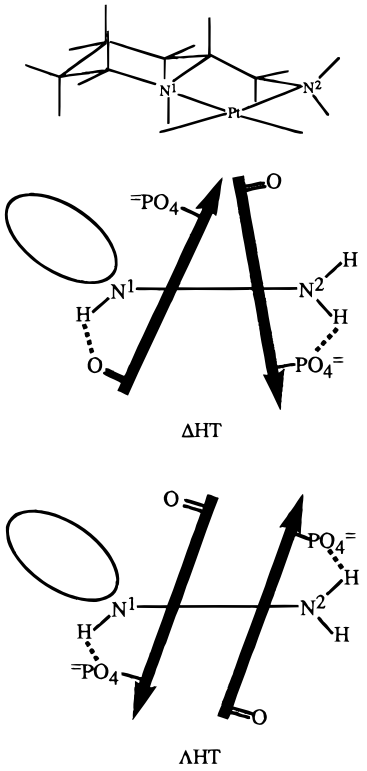

[a] Arrows are described in Chart 1 and Figure 1 captions. Dashed lines indicate likely hydrogen bonds.

3) or by its through-space effect. The observed increased population of the ΛHT atropisomer accompanying deprotonation of the phosphate group (Figure 8) is consistent with such an $ROPO_3$−HN^1 hydrogen bond.

The lower pK_a's of phosphate groups of purine 5′-nucleotides coordinated to platinum have been attributed either to hydrogen bonding between the phosphate group and an amine hydrogen[10,11,34] or to the electrostatic effect of the positively charged platinum.[46] Three of the phosphate groups in the two (*S*,*R*)-**pipen**Pt(5′-GMP)$_2$ atropisomers had the typical decrease in pK_a vs free 5′-GMP.[45] However, one of the four phosphate groups exhibited only a small decrease. This result can be readily rationalized if this one group belongs to the 5′-GMP cis to the pip ring in the ΔHT conformer; no $ROPO_3$−NH(**pipen**) hydrogen bond can readily form in this case (Chart 3). Through-space electrostatic effects should be comparably strong in all cases, so this result is less readily attributable to electrostatic effects. A recent molecular mechanics study[47] on (*R*,*S*,*S*,*R*)-**Me$_2$DAB**Pt(5′-GMP)$_2$ indicated that each phosphate group is close enough to the six-membered ring of the other 5′-GMP to form phosphate−NH(**G**) hydrogen bonds; such hydrogen bonding could decrease the pK_a. However, the observation that only one of the four pK_a's was not affected suggests that such internucleotide hydrogen bonding is not highly significant in this case. It is interesting that this finding for a ΔHT form is consistent with the evidence suggesting that the reason the ΛHT form is favored by 5′-GMP is a more favorable internucleotide interaction in the ΛHT form.

The relative influence on conformer distribution of different 5′-GMP hydrogen-bonding groups will depend on pH. At low pH, the phosphate group and the six-membered **G** ring are both protonated, and as noted, the hydrogen-bonding abilities of the PO_4 and **G** O6 groups are weak, with other factors controlling the distribution. In the neutral pH range, the PO_4 group is partly or fully deprotonated and becomes a better hydrogen-bonding group. At still higher pH, the N1H in the six-membered **G** ring becomes deprotonated and **G** O6 becomes a better hydrogen-bonding group. However, when the N9 substituent contains a phosphate group, strong **G**−**G** electrostatic effects between the charged six-membered ring (when N1H becomes deprotonated) and the dinegative phosphate groups may dominate over the effects of hydrogen bonding or steric interactions between **G** and the diamine. These considerations of the changes in **G** protonation state largely explain the dependence of the atropisomer distribution on pH. However, another factor, **G** base tilting, is also relevant; furthermore, tilting helps us to rationalize the changes in shifts as the atropisomers redistribute.

We first consider tilt in C_2-symmetrical HT adducts. In the solid state, HT forms cluster into two groups differing in tilt;[48] i.e., the bases can have either a right-handed (R) or a left-handed (L) tilt, illustrated in Chart 2. It should be noted that the degree of tilting can also be different from case to case. Relative to the average H8 signal, a lesser tilt gives less shielding and hence a deshielded (d) H8 signal, and the greater tilt gives a shielded (s) H8 signal. In theory, three sets of two variables lead to eight possible HT forms, but computations[48] on *cis*-Pt$(NH_3)_2$(guanine)$_2$ indicate that there are only four stable HT forms, as follows: ΔHTRd, ΔHTLs, ΛHTRs, and ΛHTLd. The consequences of this tilting on the NMR spectra[36,48] and on the CD spectra[36] of complexes have been analyzed.

A similar analysis can be used to interpret the (*S*,*R*)-**pipen**Pt(5′-GMP)$_2$ NMR spectra; however, one must consider separately the likely tilt of each **G** base since there is no C_2 symmetry in this case. We begin by classifying the four H8 signals into three groups depending on how the shift changed with pH as follows: (i) $\mathbf{G_A}$; (ii) $\mathbf{G_B}$ and $\mathbf{G_D}$; and (iii) $\mathbf{G_C}$. The H8 of $\mathbf{G_A}$ was relatively unaffected by pH. $\mathbf{G_D}$ (the partner of $\mathbf{G_A}$) and $\mathbf{G_B}$ have H8 signals that shifted from upfield to downfield and then back upfield as the pH was raised. Both $\mathbf{G_D}$ and $\mathbf{G_B}$ are cis to the primary amine in their respective atropisomer. $\mathbf{G_C}$ (the partner of $\mathbf{G_B}$) has an H8 signal that shifted moderately with pH, but only upfield. Thus, the H8 signals of the **G**'s cis to the secondary amine ($\mathbf{G_A}$ and $\mathbf{G_C}$) shift the least with pH.

In Chart 4, we explain the reason for these shift behaviors as a function of pH with the type of representation introduced above for the ΛHT atropisomer. Note first that $\mathbf{G_A}$ H8 (tip of arrow) is always away from $\mathbf{G_D}$, regardless of any tilt changes in $\mathbf{G_D}$. Thus, $\mathbf{G_A}$ H8 is downfield and affected little by pH changes. The H8 of $\mathbf{G_D}$, on the other hand, is affected by $\mathbf{G_A}$ anisotropy at low pH because of its tilt caused by the suspected $\mathbf{G_D}$ O6−NH(**pipen**) hydrogen bonding. At higher pH (∼7 to 8), the phosphate is deprotonated and the $\mathbf{G_D}$ tilt changes; the greater distance of $\mathbf{G_D}$ H8 from $\mathbf{G_A}$ leads to a downfield shift. Finally, at higher pH, the $\mathbf{G_D}$ six-membered ring N1H deprotonates, probably again favoring $\mathbf{G_D}$ O6−NH(**pipen**) hydrogen bonding. The tilt change brings $\mathbf{G_D}$ H8 close to $\mathbf{G_A}$, leading to the upfield shift of the $\mathbf{G_D}$ H8 signal.

In the Δ atropisomer, exactly the same sequence of tilt changes can be expected for $\mathbf{G_B}$ as depicted for $\mathbf{G_D}$ in Chart 4 for the Λ atropisomer. However, in this case the base of the

(46) Song, B.; Oswald, G.; Bastian, M.; Sigel, H.; Lippert, B. *Met.-Based Drugs* **1996**, *3*, 131.
(47) Yao, S.; Plastaras, J. P.; Marzilli, L. G. *Inorg. Chem.* **1994**, *33*, 6061.
(48) Kozelka, J.; Fouchet, M.; Chottard, J. *Eur. J. Biochem.* **1992**, *205*, 895.

Chart 4. Sketches of the ΛHT Atropisomer of (*S,R*)-**Pipen**Pt(5′-GMP)$_2$ at Different pH Values[a]

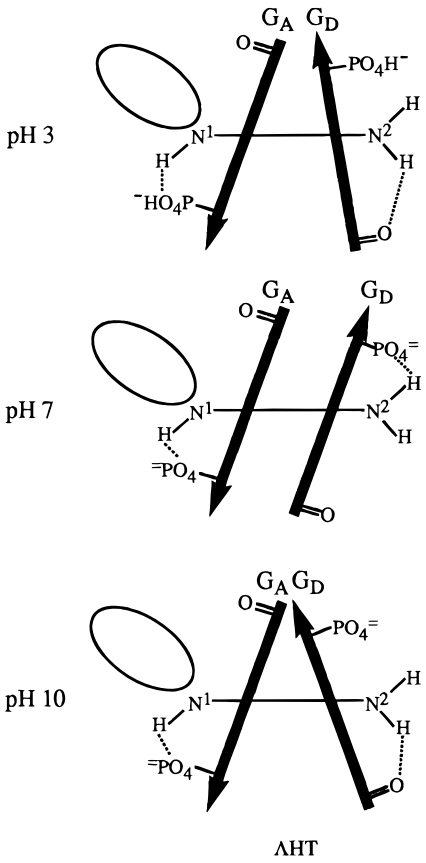

[a] The hydrogen-bonding changes with pH are shown; these explain why the tilt of $\mathbf{G_D}$ and hence $\mathbf{G_D}$ H8 shift change dramatically with pH whereas the tilt of $\mathbf{G_A}$ remains unchanged.

5′-GMP cis to the secondary amine ($\mathbf{G_C}$) is always tilted toward $\mathbf{G_B}$ and the $\mathbf{G_C}$ H8 signal is always upfield. We do not have at this time a detailed specific explanation for the further upfield shift of the G_C H8 signal with pH, but the ring anisotropy should change on N1H deprotonation.

It is tempting to speculate that the change in the atropisomer ratios is due entirely to the differences in hydrogen bonding. From ongoing studies, we believe that hydrogen bonding involving the diamine has little effect on atropisomer distribution at low pH; a protonated 5′-phosphate group or an O6 on a neutral six-membered ring of a **G** base is found on the same side of the coordination plane as NH with about equal frequency. However, near neutral pH, the deprotonated 5′-phosphate group definitely seems to favor atropisomers in which the phosphate group is close to a diamine NH; the high ratio of the Λ form (signals A and D, Figure 8) to the Δ form (signals B and C) near pH 8 is consistent with this trend and suggestive of phosphate−NH(**pipen**) hydrogen bonding.

At still higher pH, the Δ form becomes relatively more favored; this finding agrees with the suggestion that an O6 of an N1H-deprotonated, negative, six-membered **G** ring should be a better NH hydrogen-bonding acceptor group. However, it is also possible that the Δ form is favored because of mutual attractive and/or repulsive forces between the trinegative 5′-GMP ligands. More studies are needed before factors influencing distribution in this very high pH range become clear.

Finally, we consider the relationship between atropisomer interconversion rate and the properties of the carrier ligand, including the chelate ring size and the substituents on the amine groups. **G** bases coordinated to platinum complexes with nonbulky amine groups, such as $(NH_3)_2$ (cisplatin) and **en** (ethylenediamine), exhibit fast rotation around the Pt−N7 bond on the NMR time scale.[27−32] For complexes with a six-membered chelate ring, several conformations, including chair, skew, and boat, can be adopted. This additional flexibility results in low-energy structures with axial *N*-methyl groups, according to molecular mechanics and dynamics calculations on **Me$_2$-DAP**Pt$\mathbf{G}_2$ complexes[45,49] (**Me$_2$DAP** = *N,N*′-dimethyl-2,4-diaminopentane). Rapid rotation about the Pt−N7 bond is generally observed. Five-membered chelate rings with two asymmetric carbons are less flexible; generally, at least one *N*-alkyl substituent is equatorial to minimize intraligand steric repulsions. Thus, **Me$_2$DAB**Pt$\mathbf{G}_2$ complexes[7,8,37] atropisomerize more slowly than **Me$_2$DAP**Pt$\mathbf{G}_2$ complexes.[45,49] However, EXSY cross-peaks in the spectra of **Me$_2$DAB**Pt$\mathbf{G}_2$ complexes[7,8,37] showed that all atropisomers interchange even at 5 °C. In **Bip**Pt$\mathbf{G}_2$ complexes, the rigid amine makes rotation around the Pt−N7 bond very slow, such that not only are there no EXSY peaks but there is no magnetization transfer even at 80 °C.[35] Thus, even when the carrier ligand permits observation of different atropisomers, the dynamic properties can vary.

For the **pipen**Pt$\mathbf{G}_2$ complexes studied here, the diamine ligand is a hybrid, having a more rigid bulky pip moiety on one side and a nonbulky primary amine on the other side. The **pipen** ligand can hinder rotation of the 5′-GMP cis to the secondary amine. Interconversion from one HT isomer to the other requires rotation of both 5′-GMP's. If one 5′-GMP is strongly hindered in its rotation, the overall rate of interconversion of one HT isomer into the other would be slow. This is why we did not observe exchange between atropisomers in the NOESY/EXSY experiment at 5 °C. The reasonably sharp 1D NMR signals of individual HT atropisomers observed at room temperature indicate slow exchange. However, if the rotation of the 5′-GMP cis to the primary amine is fast, the interconversion between a given HT isomer and one HH isomer would be fast. Then, the HH isomers may contribute to some extent to the resonances assigned to each HT isomer. The fact that there was no H8−H8 NOE cross-peak for either atropisomer indicates that the populations of any HH isomers are very low.

At higher pH, the H8 signals for the **G**'s cis to the primary amine ($\mathbf{G_D}$ in ΛHT and $\mathbf{G_B}$ in ΔHT) clearly broaden (Figure 8). If the broadening were due to more rapid interconversion between ΔHT and ΛHT, all H8 signals would have broadened. The H8 signals of $\mathbf{G_A}$ and $\mathbf{G_C}$ remain sharp and do not appear to be very sensitive to the broadening process, which may be localized to the **G**'s cis to the primary amine of each atropisomer. We suspect that the results are consistent with a relatively fixed **G** next to the secondary amine, but further work at lower temperatures in mixed solvents may be needed to determine the cause of the broadening.

The dynamic processes that we believe are occurring in the acidic to neutral pH range are shown in Figure 1. The most abundant form, ΛHT, is in rapid equilibration with a trace amount of HH_1. ΛHT equilibrates slowly with ΔHT, which equilibrates rapidly with trace amounts of HH_2. Qualitatively, the ΔHT to ΛHT atropisomerization rate is probably influenced by the amine ligand(s) in the following order: $(NH_3)_2 \sim$ **en** > **Me$_2$DAP** > **Me$_2$DAB** ≫ **pipen** > **Bip**.

(49) Cerasino, L.; Williams, K. M.; Intini, F. P.; Cini, R.; Marzilli, L. G.; Natile, G. *Inorg. Chem.* **1997**, *36*, 6070.

Conclusions

We conclude that the configuration of the secondary amine is the single most important determinant of **G** base orientation. In the **pipen** complexes, where only one secondary amine is present, the effect is modulated. Furthermore, the pipen complexes are more dynamic than those with the **Bip** carrier ligand, which has two secondary amines incorporated into pip rings. However, the one pip ring in **pipen** can decrease the ΔHT to ΛHT interconversion rate compared to the **Me$_2$DAB** carrier ligand. Nevertheless, the latter is more stereocontrolling than **pipen**, and it appears that dynamic motions and stereocontrol are not strongly coupled. Such a decoupling of dynamic reactivity and stereocontrol could possibly be exploited in the design of anticancer drugs. Indeed, the derivatives of anticancer drugs are too dynamic for an assessment of the interactions of the **G** with the cis amine. However, the hybrid nature of the **pipen** ligand allowed us to evaluate the interactions of the **G** derivative with a cis primary amine. This **G** is within an environment similar to that for the anticancer drugs, which are generally more active with primary than with secondary amine carrier ligands. Experiments between **pipen** and other G derivatives are discussed in another paper.[50]

Our new results are useful for understanding the CD spectra of *cis*-PtA$_2$**G**$_2$ species. The pH jump experiment demonstrates that, in this case, the sign of the CD signal reflects the absolute conformation of the major HT atropisomer, even though CD signal intensities reflect the sum of the signals of all species. Cisplatin−DNA adducts exhibit dramatically enhanced CD signal intensity,[51−54] and Pt derivatives with stereocontrolling ligands such as **pipen** or **Bip** may prove to be helpful aids in understanding the origins of these large CD effects.

Acknowledgment. This work was supported by NIH Grant GM 29222 (to L.G.M.) and NATO CRG. 950376 (to L.G.M. and G.N.); and MURST (contribution 40%), CNR, and EC (COST Chemistry Project D8/0012/97 (to G.N.).

Supporting Information Available: Table of analytical data for **pipen**·2HCl and PtX$_2$(**pipen**) and figures of the COSY spectrum of **pipen**·2HCl, the NOESY spectrum of (*S*,*R*)-**pipen**Pt(5′-GMP)$_2$, the H8 ^{1}H NMR signals of (*S*,*R*)-pipenPt(5′-GMP)$_2$ at various pH values, and the CD spectrum of (*S*,*R*)-Pt(NO$_3$)$_2$(**pipen**). This material is available free of charge via the Internet at http://pubs.acs.org.

IC980987U

(50) Wong, H. C.; Intini, F. P.; Natile, G.; Marzilli, L. G. *Inorg. Chem.*, in press.

(51) Macquet, J.; Butour, J. *Eur. J. Biochem.* **1978**, *83*, 375.

(52) Srivastava, R. C.; Froehlich, J.; Eichhorn, G. L. *Biochimie* **1978**, *60*, 879.

(53) Navarro-Ranninger, C.; López-Solera, I.; Pérez, J. M.; Rodríguez, J.; García-Ruano, J. L.; Raithby, P. R.; Masaguer, J. R.; Alonso, C. *J. Med. Chem.* **1993**, *36*, 3795.

(54) Quiroga, A. G.; Pérez, J. M.; López-Solera, I.; Masaguer, J. R.; Luque, A.; Román, P.; Edwards, A.; Alonso, C.; Navarro-Ranninger, C. *J. Med. Chem.* **1998**, *41*, 1399.